Correspondence

Segmentation of Magnetic Resonance Images Using Fuzzy Algorithms for Learning Vector Quantization

Nicolaos B. Karayiannis* and Pin-I Pai

***Abstract*—This paper evaluates a segmentation technique for magnetic resonance (MR) images of the brain based on fuzzy algorithms for learning vector quantization (FALVQ). These algorithms perform vector quantization by updating all prototypes of a competitive network through an unsupervised learning process. Segmentation of MR images is formulated as an unsupervised vector quantization process, where the local values of different relaxation parameters form the feature vectors which are represented by a relatively small set of prototypes. The experiments evaluate a variety of FALVQ algorithms in terms of their ability to identify different tissues and discriminate between normal tissues and abnormalities.**

***Index Terms*—Fuzzy algorithms for learning vector quantization, learning vector quantization, magnetic resonance imaging, segmentation.**

I. Introduction

The clinical utility of magnetic resonance (MR) imaging rests on the contrasting image intensities obtained for different tissue types; both normal and abnormal. For a given MR-image pulse sequence, image intensities will depend on local values of the following relaxation parameters: the spin-lattice relaxation time (T1), the spin-spin relaxation time (T2), and the spin density (SD). Recent trends in diagnostic radiology have placed an emphasis on computer-based image segmentation techniques. The existence of computationally efficient and reliable MR-image segmentation techniques can enhance the ability of radiologists to detect, diagnose, and monitor pathology.

Image segmentation is the process of selectively eliminating the redundancy that is naturally present in images. In general, image segmentation is accomplished by dividing an image into segments with uniform and homogeneous attributes, such as tone and texture [6]. In the context of MR imaging, segmentation is the process of selectively removing the redundancy present in MR images without affecting the details that play a key role in the diagnostic process. The utility of segmented MR images in the medical diagnostic process depends on the combination of two, often conflicting, requirements, that is, the elimination of the redundant information present in the original MR images and the preservation of the important details in the resulting segmented images. MR-image segmentation techniques are often evaluated in terms of their ability to 1) differentiate between cerebro-spinal fluid (CSF), white matter, and gray matter and 2) differentiate between normal tissues and abnormalities.

The development of MR-image segmentation techniques has been attempted in recent years using classical pattern recognition methods, rule-based systems, image analysis methods, crisp and fuzzy clustering procedures, and feed-forward neural networks. Hyman *et al.* [8] used a maximum likelihood method for classifying normal brain tissue. This approach was used for the analysis of MR images of 45 volunteers and achieved a discrimination accuracy of 84% for 13 tissue types among three age groups, with classification accuracy for individual regions ranging from 50 to 100%. Raya [19] presented a rule-based system for low-level segmentation of MR brain images. In this approach, the proton-density and T2-weighted parameters were used to separate voxels of different structures. The segmentation process was based on a set of heuristics which were coded into a set of rules. Since rule-based systems are problem specific, the rules proposed in this paper are applicable only to the imaging protocol used [19]. For a different imaging protocol a different set of rules must be formulated. The task of formulating new rules involves studying statistical properties of voxels of different structures, formulating segmentation heuristics, and coding the heuristics into rules. Bomans *et al.* [2] combined edge-detection operators and morphological filtering for segmentation and reconstruction of anatomical surfaces from MR-image data. An extension of the Marr–Hildreth operator [7] was used for edge detection. Morphological filters, dilation, and erosion, were subsequently applied to refine the detected edges and improve the surface definition [21]. Clarke [3] compared a maximum likelihood method with a neural-network technique for tissue classification. The two approaches were tested on idealized and nonidealized image data, all obtained with phantoms for image standardization. Imaged subjects included healthy volunteers and selected patients with brain tumors undergoing radiation therapy. In this study, neural networks provided better boundary definition for nonidealized data [3]. Hall *et al.* [5] compared MR-image segmentation techniques based on supervised multilayered neural networks [20] and the unsupervised fuzzy c-means algorithm [1]. These segmentation techniques were tested on MR images from healthy volunteers and selected patients with brain tumors surrounded by edema. The supervised and unsupervised segmentation techniques used in this study produced broadly similar results. Inconsistency of ratings among experts was observed in a complex segmentation problem with tumor/edema or CSF boundary where tissues have similar MR-relaxation behavior [5].

MR-image segmentation techniques based on statistical approaches require *a priori* statistical assumptions which are rarely satisfied in practice. The development of a flexible rule-based MR-image segmentation system with the ability to generalize requires a computationally complex and time consuming rule-production system. The implementation of a reliable MR-image segmentation system based on the aforementioned image analysis techniques requires the fine tuning of the parameters determining the Gaussian function which is convolved with the image, the size of the filtering and edge-detection windows, and the size and shape of the structuring element used in morphological operators. Finally, MR-image segmentation based on feed-forward neural networks relies heavily on the training set used for their supervised training. The training set is constructed by selecting feature vectors from a single MR image or an ensemble of MR images and reflects the judgment of the human expert(s) who assign labels to the feature vectors according to the tissues they represent.

Segmentation of MR images is formulated in this study as the problem of partitioning a set of feature vectors obtained from an MR

Manuscript received September 11, 1996; revised January 8, 1999. The Associate Editor responsible for coordinating the review of this paper and recommending its publication was M. Vannier. *Asterisk indicates corresponding author*.

*N. B. Karayiannis is with the Department of Electrical and Computer Engineering, University of Houston, Houston, TX 77204-4793 USA.

P.-I. Pai is with TransComm Technology System, Inc., Fremont, CA 94538 USA.

Publisher Item Identifier S 0278-0062(99)03150-X.

0278–0062/99$10.00 © 1999 IEEE

image into a relatively small number of clusters, each represented by a vector called the prototype. Each feature vector contains as elements the T1, T2, and SD parameters at a certain image location. Following the learning vector quantization process used to form a partition of the feature vectors, the segmented image is obtained by representing each feature vector by its closest prototype. As a result, the segmented image contains a number of segments equal to the number of prototypes, which is much smaller than the number of intensity levels in the original MR image.

II. Learning Vector Quantization

The objective of vector quantization (VQ) is the representation of a set of vectors $\mathbf{x} \in \mathcal{X} \subset \mathbb{R}^n$ by a set of c prototypes $\mathcal{V} = \{\mathbf{v}_1, \mathbf{v}_2, \cdots, \mathbf{v}_c\} \subset \mathbb{R}^n$. Thus, VQ can also be seen as a mapping from an n-dimensional Euclidean space into the finite set $\mathcal{V} \in \mathbb{R}^n$, also referred to as the codebook. Codebook design can be performed by clustering algorithms, which are typically developed by solving a constrained minimization problem using alternating optimization. These clustering techniques include the crisp c-means [4], fuzzy c-means [1], generalized fuzzy c-means [9], and entropy-constrained fuzzy clustering algorithms [11]. Clustering algorithms can be divided into crisp and fuzzy, depending on the strategy they employ for assigning feature vectors into clusters during the clustering process. Crisp clustering algorithms assign each feature vector to a single cluster. Thus, the partition of the feature vector space is based on crisp or hard decisions. Fuzzy clustering algorithms consider each cluster as a fuzzy set, while each feature vector is assigned to multiple clusters as indicated by a membership function. Thus, the partition of the feature vector space is based on soft decisions. Fuzzy clustering algorithms outperform crisp clustering algorithms, which are susceptible to local minima and depend rather strongly on the initialization of the clustering process.

Recent developments in neural network architectures resulted in learning vector quantization (LVQ) algorithms [10]. LVQ is the name used for unsupervised learning algorithms associated with the competitive network shown in Fig. 1. The network consists of an input layer and an output layer. Each node in the input layer is connected with the cells, or units, in the output layer as shown in Fig. 1. Kohonen [17] proposed an unsupervised learning scheme, known as the (unlabeled data) LVQ. This algorithm can be used to generate crisp c partitions of unlabeled data vectors. Pal *et al.* [18] identified a close relationship between this algorithm and a clustering procedure, proposed earlier by MacQueen, known as the sequential hard c-means algorithm. Tsao *et al.* [22] proposed a batch learning scheme, known as fuzzy LVQ (FLVQ). Karayiannis and Bezdek [14] derived a broad family of batch LVQ algorithms that can be implemented as the fuzzy c-means or the FLVQ algorithms. Pal *et al.* [18] suggested that LVQ can be performed through an unsupervised learning process, using a competitive neural network whose weight vectors represent the prototypes. This formulation resulted in the generalized LVQ (GLVQ) algorithm [18]. The GLVQ-F algorithms were then developed in an attempt to overcome scaling problems associated with the original GLVQ algorithm [13]. Karayiannis and Pai [12], [15], [16] proposed a framework for the development of fuzzy algorithms for LVQ (FALVQ). This formulation resulted in the development of a broad variety of FALVQ algorithms, which are distinguished by the different strategies they employ to regulate the competition between the prototypes during the learning process.

LVQ algorithms can be grouped using as criterion the prototypes updated to match the inputs of the LVQ network. Crisp LVQ algorithms allow the update of only the winning prototype, that is, the closest prototype to the input of the LVQ competitive network. Soft LVQ algorithms allow all prototypes to be updated in order to match the input of the LVQ network. LVQ algorithms can also be grouped on the basis of the learning strategy they employ. In batch LVQ algorithms the prototypes are updated after all input vectors are presented simultaneously to the LVQ network. In sequential LVQ algorithms the prototypes are updated to match each one of the input vectors which are presented sequentially to the LVQ competitive network. Table I shows the majority of the existing families of LVQ algorithms, classified according to the criteria mentioned above.

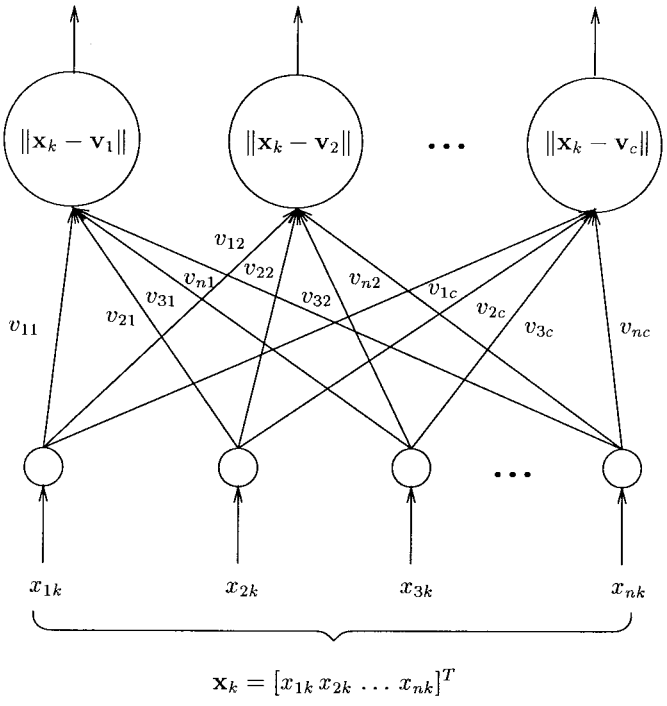

Fig. 1. An LVQ competitive network.

TABLE I
Classification of Learning Vector Quantization Algorithms

	Batch Updates	Sequential Updates
Crisp Learning	–	LVQ
Soft Learning	FLVQ	GLVQ, GLVQ-F & FALVQ

A. FALVQ

Consider the set $\mathcal{X}$ of samples from an n-dimensional Euclidean space and let $f(\mathbf{x})$ be the probability distribution function of $\mathbf{x} \in \mathcal{X} \subset \mathbb{R}^n$. LVQ is frequently based on the minimization of the functional [18]

$$L(\mathbf{v}_1, \mathbf{v}_2, \cdots, \mathbf{v}_c) = \iint \cdots \int_{\mathbb{R}^n} \sum_{r=1}^{c} u_r(\mathbf{x}) \|\mathbf{x} - \mathbf{v}_r\|^2 f(\mathbf{x})\, d\mathbf{x} \tag{1}$$

which represents the expectation of the loss function $L_{\mathbf{x}} = L_{\mathbf{x}}(\mathbf{v}_1, \mathbf{v}_2, \cdots, \mathbf{v}_c)$, defined as

$$L_{\mathbf{x}}(\mathbf{v}_1, \mathbf{v}_2, \cdots, \mathbf{v}_c) = \sum_{r=1}^{c} u_r(\mathbf{x}) \|\mathbf{x} - \mathbf{v}_r\|^2. \tag{2}$$

In the above definitions, $u_r(\mathbf{x}), 1 \leq r \leq c$ represent membership functions that regulate the competition between the prototypes $\mathbf{v}_r, 1 \leq r \leq c$ for the input $\mathbf{x}$. The specific form of the membership functions determines the strength of attraction between each input

and the prototypes during the learning process [12], [16]. The loss function is often defined with respect to the winning prototype. Assuming that $\mathbf{v}_i$ is the winning prototype corresponding to the input vector $\mathbf{x}$, that is, the closest prototype to $\mathbf{x}$ in the Euclidean distance sense, the memberships $u_{ir} = u_r(\mathbf{x})$, $1 \le r \le c$, can take the form

$$u_{ir} = \begin{cases} 1, & \text{if } r = i \\ u\left(\dfrac{\|\mathbf{x}-\mathbf{v}_i\|^2}{\|\mathbf{x}-\mathbf{v}_r\|^2}\right), & \text{if } r \neq i. \end{cases} \tag{3}$$

In such a case, the loss function (2) measures the locally weighted error of each input vector with respect to the winning prototype [18]. Pal *et al.* [18] suggested that (1) can be minimized by using the gradient of the instantaneous loss function (2) when the probability distribution function $f(\cdot)$ is not known. This approach implies the sequential update of the prototypes with respect to the input vectors $\mathbf{x} \in \mathcal{X}$.

If $u_{ir} = 0, \forall r \neq i$, then minimization of the loss function (2) using gradient descent leads to Kohonen's (unlabeled data) LVQ [17], which can be used to generate crisp c partitions of unlabeled data vectors. According to this learning scheme, only the winning prototype is updated during learning to match the input vector. Because of the inherent bias toward the winning prototype, Kohonen's (unlabeled data) LVQ depends strongly on the initial set of prototypes and is susceptible to local minima.

The development of FALVQ algorithms requires the selection of the membership functions assigned to the prototypes [12], [16]. A fair competition among the prototypes is guaranteed if the membership function assigned to each prototype: 1) is invariant under uniform scaling of the entire data set; 2) is equal to one if the prototype is the winner; 3) takes values between one and zero if the prototype is not a winner; and 4) approaches zero if the prototype is not a winner and its distance from the input vector approaches infinity.

A variety of FALVQ algorithms can be derived by minimizing the loss function using gradient descent. If $\mathbf{x}$ is the input vector, the winning prototype $\mathbf{v}_i$ can be updated by [12], [16]

$$\Delta\mathbf{v}_i = \eta(\mathbf{x}-\mathbf{v}_i)\left(1 + \sum_{r\neq i}^{c} w_{ir}\right) \tag{4}$$

where η is the learning rate and $w_{ir} = w(\|\mathbf{x}-\mathbf{v}_i\|^2/\|\mathbf{x}-\mathbf{v}_r\|^2)$ with

$$w(z) = u'(z). \tag{5}$$

Each nonwinning prototype $\mathbf{v}_j \neq \mathbf{v}_i$ can be updated by [12], [16]

$$\Delta\mathbf{v}_j = \eta(\mathbf{x}-\mathbf{v}_j)n_{ij} \tag{6}$$

where $n_{ij} = n(\|\mathbf{x}-\mathbf{v}_i\|^2/\|\mathbf{x}-\mathbf{v}_j\|^2)$ with

$$n(z) = u(z) - zu'(z). \tag{7}$$

The update of the prototypes depends on the learning rate $\eta \in [0, 1]$, which is a monotonically decreasing function of the number of iterations ν. The learning rate can be a linear function of ν defined as $\eta = \eta(\nu) = \eta_0(1-\nu/N)$, where η_0 is its initial value and N the total number of iterations predetermined for the learning process.

The above formulation provided the basis for the development of the FALVQ 1, FALVQ 2, and FALVQ 3 families of algorithms [12], [16]. Table II shows the membership functions $u(\cdot)$ that generated these families of algorithms and the corresponding interference functions $w(\cdot)$ and $n(\cdot)$. If $\mathbf{x}$ is the input vector, then the winning prototype is updated by (4), with w_{ir} evaluated in terms of the interference function $w(\cdot)$ shown in Table II as $w_{ir} = w(\|\mathbf{x}-\mathbf{v}_i\|^2/\|\mathbf{x}-\mathbf{v}_r\|^2)$. The nonwinning prototypes $\mathbf{v}_j \neq \mathbf{v}_i$ can be updated by (6), with n_{ij} evaluated in terms of the interference function $n(\cdot)$ shown in Table II as $n_{ij} = n(\|\mathbf{x}-\mathbf{v}_i\|^2/\|\mathbf{x}-\mathbf{v}_j\|^2)$.

TABLE II
MEMBERSHIP FUNCTIONS AND INTERFERENCE FUNCTIONS FOR THE FALVQ 1, FALVQ 2, AND FALVQ 3 FAMILIES OF ALGORITHMS

FALVQ Family	$u(x)$	$w(x)$	$n(x)$
FALVQ 1 $(0<\alpha<\infty)$	$x(1+\alpha x)^{-1}$	$(1+\alpha x)^{-2}$	$\alpha x^2(1+\alpha x)^{-2}$
FALVQ 2 $(0<\beta<\infty)$	$x\exp(-\beta x)$	$(1-\beta x)\exp(-\beta x)$	$\beta x^2\exp(-\beta x)$
FALVQ 3 $(0<\gamma<1)$	$x(1-\gamma x)$	$1-2\gamma x$	γx^2

The update of the winning prototype is affected by the term $1 + \sum_{r\neq i}^{c} w_{ir}$, which depends on the number of prototypes. The effect of the number of prototypes on the performance of FALVQ algorithms can be moderated by replacing in the update equations (4) and (6) the learning rate η by $\eta/(1+\hat{w}(c-1))$ where $\hat{w} = \hat{w}(\nu)$ increases linearly with the iteration number ν from its minimum value $\hat{w}_{\min}$ to its maximum value $\hat{w}_{\max}$ as

$$\hat{w} = \hat{w}_{\min} + \nu(\hat{w}_{\max} - \hat{w}_{\min})/N. \tag{8}$$

The minimum value $\hat{w}_{\min}$ of $\hat{w}$ can be determined by observing that the interference function w_{ir} attains its minimum value if $\|\mathbf{x}-\mathbf{v}_r\|^2 \approx \|\mathbf{x}-\mathbf{v}_i\|^2$, $\forall r \neq i$, which is more likely to occur in the beginning of the learning process. It is also reasonable to expect that near the end of learning process $\|\mathbf{x}-\mathbf{v}_r\|^2 \gg \|\mathbf{x}-\mathbf{v}_i\|^2$, $\forall r \neq i$, which implies that the interference function w_{ir} attains its maximum value. Typical values for $\hat{w}_{\min}$ and $\hat{w}_{\max}$ can be obtained from the extreme values of the interference function corresponding to the FALVQ 1 algorithm with $\alpha = 1$. In this case, the condition $\|\mathbf{x}-\mathbf{v}_r\|^2 \approx \|\mathbf{x}-\mathbf{v}_i\|^2$ implies that $w_{ir} \approx 1/4$, while the condition $\|\mathbf{x}-\mathbf{v}_r\|^2 \gg \|\mathbf{x}-\mathbf{v}_i\|^2$ implies that $w_{ir} \approx 1$.

The resulting FALVQ algorithms can be summarized as follows.

1) Select c; fix η_0, N; set $\nu = 0$; randomly generate an initial codebook $\mathcal{V}_0 = \{\mathbf{v}_{1,0}, \mathbf{v}_{2,0}, \ldots, \mathbf{v}_{c,0}\}$.
2) Calculate $\eta = \eta_0(1-\nu/N)/(\hat{w}_{\min} + \nu(\hat{w}_{\max} - \hat{w}_{\min})/N)$.
3) Set $\nu = \nu + 1$.
4) For each input vector $\mathbf{x}$:

   find i such that $\|\mathbf{x}-\mathbf{v}_{i,\nu-1}\|^2 < \|\mathbf{x}-\mathbf{v}_{j,\nu-1}\|^2$, $\forall j \neq i$;
   calculate $u_{ir,\nu} = u(\|\mathbf{x}-\mathbf{v}_{i,\nu-1}\|^2/\|\mathbf{x}-\mathbf{v}_{r,\nu-1}\|^2)$, $\forall r \neq i$;
   calculate $w_{ir,\nu} = u'(\|\mathbf{x}-\mathbf{v}_{i,\nu-1}\|^2/\|\mathbf{x}-\mathbf{v}_{r,\nu-1}\|^2)$, $\forall r \neq i$;
   calculate $n_{ir,\nu} = u_{ir,\nu} - (\|\mathbf{x}-\mathbf{v}_{i,\nu-1}\|^2/\|\mathbf{x}-\mathbf{v}_{r,\nu-1}\|^2)w_{ir,\nu}$, $\forall r \neq i$;
   update $\mathbf{v}_i$ by $\mathbf{v}_{i,\nu} = \mathbf{v}_{i,\nu-1} + \eta(\mathbf{x}-\mathbf{v}_{i,\nu-1})(1+\sum_{r\neq i}^{c} w_{ir,\nu})$;
   update $\mathbf{v}_j \neq \mathbf{v}_i$ by $\mathbf{v}_{j,\nu} = \mathbf{v}_{j,\nu-1} + \eta(\mathbf{x}-\mathbf{v}_{j,\nu-1})n_{ij,\nu}$.

5) If $\nu < N$, then go to step 2.

B. Competition Measures

The performance of FALVQ algorithms depends on the competition between the winning and nonwinning prototypes, which can be related to the form of the corresponding membership functions by the competition measures presented below [12].

According to the formulation that resulted in the FALVQ families of algorithms, the nonwinning prototypes are not updated to match the input vector if $u(z) = z$ or $u(z) = 0$, $\forall z \in (0, 1)$. It can be observed that

$$\int_0^1 u(z)\,dz = \begin{cases} \frac{1}{2}, & \text{if } u(z) = z \\ 0, & \text{if } u(z) = 0. \end{cases} \tag{9}$$

For any other membership function selected according to the proposed admissibility conditions

$$0 < \int_0^1 u(z)\,dz < \tfrac{1}{2}. \tag{10}$$

Thus, the area $A_u = \int_0^1 u(z)\,dz$ can be used as a measure of the competition between the winning and winning prototypes. The development of competitive FALVQ algorithms requires that $A_u \in (0, 1/2)$. Moreover, the nonwinning prototypes become less competitive as A_u approaches zero or $1/2$.

The competition between the winning and nonwinning prototypes during the learning process can be quantified by considering the area A_u in conjunction with the centroid or center of gravity of the membership function $u(\cdot)$. Assuming that $A_u = \int_0^1 u(z)\,dz \neq 0$, the centroid of $u(z)$ over the interval $z \in (0, 1)$ is defined as

$$C_u = \frac{\int_0^1 z u(z)\,dz}{\int_0^1 u(z)\,dz}. \tag{11}$$

The centroid (11) is a useful source of information regarding the shape of $u(\cdot)$ and, thus, the bias of the resulting FALVQ algorithm toward the winning prototype. In the extreme case where $u(z) = z$, $C_u = 2/3$. If $u(\cdot)$ is an admissible membership function, then $C_u < 2/3$. Since the selection of $u(z) = z$ implies that the nonwinning prototypes are not updated to match the input vector, the development of competitive FALVQ algorithms requires a membership function that corresponds to a centroid value lower than $2/3$. Nevertheless, the nonwinning prototypes become increasingly competitive if the centroid C_u decreases below $1/2$. If the value of C_u is sufficiently close to zero, the competition between the winning and nonwinning prototypes diminishes.

Fig. 2(a) plots the competition measures $A_u = A_u(\alpha)$ and $C_u = C_u(\alpha)$ as functions of the free parameter α involved in the definition of the membership function that led to the FALVQ 1 family. According to Fig. 2(a), $A_u(\alpha)$ attains values very close to $1/2$ for small values of α. In this case, the winning prototypes are not updated to match the input vector. As α increases, the value of $A_u(\alpha)$ decreases very slowly to zero, the other extreme value of this competition measure, which indicates that the winning prototypes are not updated to match the input vector. As the value of α increases from zero to infinity, $C_u(\alpha)$ decreases asymptotically from its maximum value of $2/3$ to $1/2$, its lower bound. Thus, the area $A_u = A_u(\alpha)$ is a more reliable competition measure for the FALVQ 1 family of algorithms.

Fig. 2(b) plots the competition measures $A_u = A_u(\beta)$ and $C_u = C_u(\beta)$ as functions of the free parameter β involved in the definition of the membership function that led to the FALVQ 2 family. According to Fig. 2(b), $A_u(\beta)$ decreases quickly to values close to zero as the value of β increases. Thus, the competition between the winning and nonwinning prototypes diminishes quickly as the values of β exceed a certain threshold. The centroid $C_u(\beta)$ can take positive values significantly lower than $1/2$ for large values of β. Such values of $C_u(\beta)$ indicate that there is practically no competition between the prototypes during the learning process. In conjunction with the area $A_u = A_u(\beta)$, $C_u(\beta)$ can be used to select the range of values of β that allow the nonwinning prototypes to compete with the winning prototype during learning.

Fig. 2(c) plots the competition measures $A_u = A_u(\gamma)$ and $C_u = C_u(\gamma)$ as functions of the free parameter $\gamma \in (0, 1]$ involved in the definition of the membership function that led to the FALVQ 3 family. According to Fig. 2(c), $A_u(\gamma)$ attains its maximum value $1/2$ for $\gamma = 0$, which corresponds to no competition, and decreases linearly from $1/2$ to $1/6$ as γ spans the interval $(0, 1]$. The competition measure $C_u(\gamma)$ decreases from $2/3$ to $1/2$ as the value of γ increases from zero to one. Since $C_u(\gamma)$ takes values higher than $1/2$ as γ spans the interval $(0, 1)$, $C_u(\gamma)$ is not a particularly informative competition measure in this case. Thus, the area $A_u = A_u(\gamma)$ can be used for selecting the values of γ for FALVQ 3 algorithms.

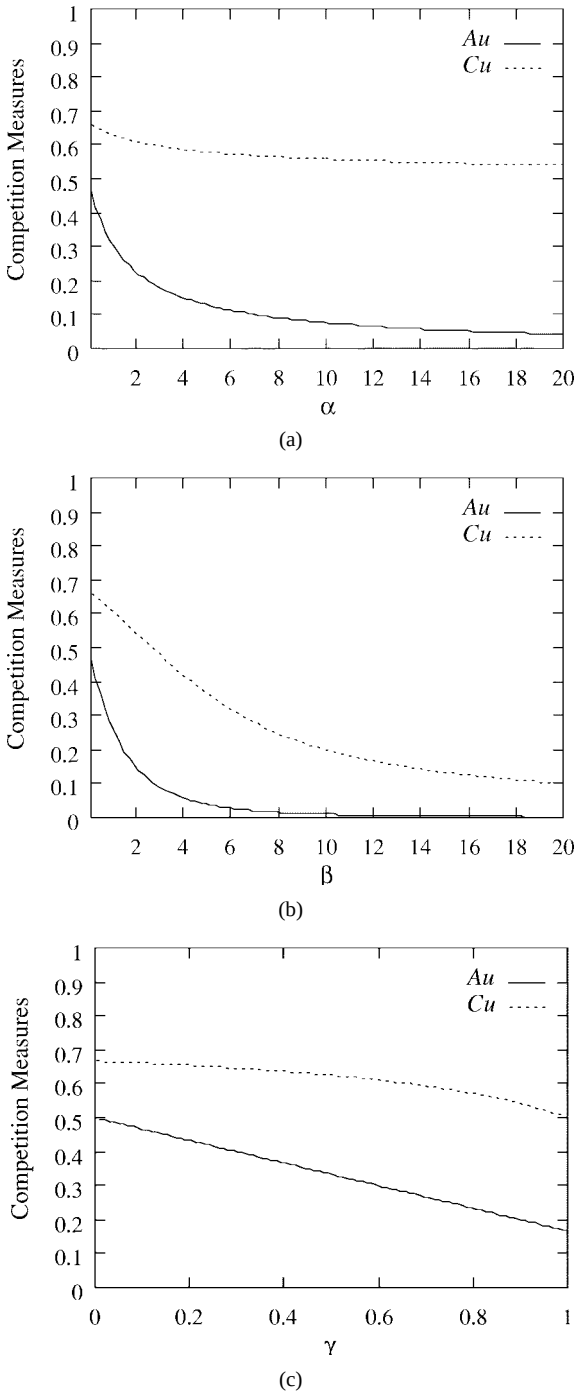

Fig. 2. Competition measures: (a) $A_u(\alpha)$ and $C_u(\alpha)$ as functions of α. (b) $A_u(\beta)$ and $C_u(\beta)$ as functions of β. (c) $A_u(\gamma)$ and $C_u(\gamma)$ as functions of γ.

C. Generalized FALVQ 1 Algorithms

The admissibility conditions proposed for the development of FALVQ algorithms are satisfied by a broad variety of membership

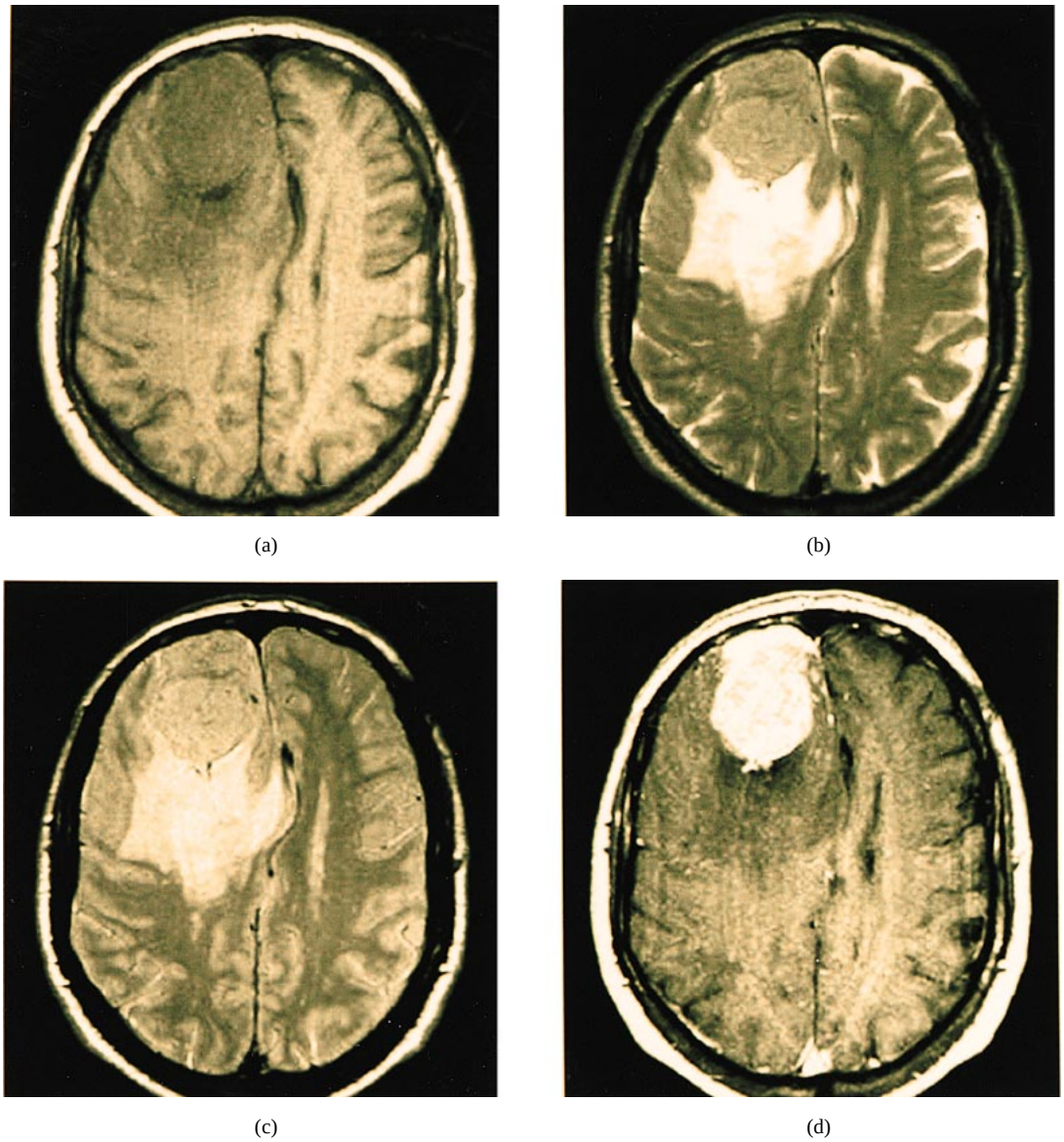

(a) (b) (c) (d)

Fig. 3. Magnetic resonance image of the brain of an individual suffering from meningioma. (a) T1-weighted image. (b) T2-weighted image. (c) Spin-density image. (d) T1-weighted image after the patient was given Gadolinium.

functions of the form [10], [15]

$$u_{ir} = \begin{cases} 1, & \text{if } r = i \\ \left(1 + \dfrac{\|\mathbf{x} - \mathbf{v}_r\|^2}{D(\mathbf{x})}\right)^{-1}, & \text{if } r \neq i \end{cases} \tag{12}$$

where $D(\mathbf{x}) = D(\|\mathbf{x} - \mathbf{v}_j\|^2, \mathbf{v}_j \in \mathcal{V})$ is a differentiable function of $\|\mathbf{x} - \mathbf{v}_j\|^2$, $\mathbf{v}_j \in \mathcal{V}$, such that

$$D(\mathbf{x}) \geq D_{\min}(\mathbf{x}) = \min_{1 \leq j \leq c} \{\|\mathbf{x} - \mathbf{v}_j\|^2\}. \tag{13}$$

A function worth investigating is the generalized mean (or unweighted p norm) $D_p(\mathbf{x})$ of $\|\mathbf{x} - \mathbf{v}_\ell\|^2$, $1 \leq \ell \leq c$, defined as

$$\begin{aligned} D_p(\mathbf{x}) &= D_p(\|\mathbf{x} - \mathbf{v}_\ell\|^2, \mathbf{v}_\ell \in \mathcal{V}) \\ &= \left(\frac{1}{c} \sum_{\ell=1}^{c} (\|\mathbf{x} - \mathbf{v}_\ell\|^2)^p\right)^{1/p} \end{aligned} \tag{14}$$

with $p \in (-\infty, 0)$.

The Generalized FALVQ 1 algorithm can be derived by using the gradient descent method to minimize the loss function (2), with $u_r(\mathbf{x}) = u_{ir}$ defined by (12) and $D(\mathbf{x}) = D_p(\mathbf{x})$. If $\mathbf{x}$ is the input vector, then the winning prototype $\mathbf{v}_i$ can be updated by [10]

$$\Delta \mathbf{v}_i = \eta(\mathbf{x} - \mathbf{v}_i)\left(1 + \frac{1}{c} \sum_{r \neq i}^{c} w_{ir}(\mathbf{v}_i)\right) \tag{15}$$

while the nonwinning prototypes $\mathbf{v}_j \neq \mathbf{v}_i$ can be updated by [10]

$$\Delta \mathbf{v}_j = \eta(\mathbf{x} - \mathbf{v}_j)\left(u_{ij}^2 + \frac{1}{c} \sum_{r \neq i}^{c} w_{ir}(\mathbf{v}_j)\right). \tag{16}$$

In the update equations (15) and (16), η is the learning rate and $w_{ir}(\mathbf{v}_\ell)$ is the interference function corresponding to the prototype $\mathbf{v}_\ell$, defined as

$$w_{ir}(\mathbf{v}_\ell) = u_{ir}^2 \left(\frac{\|\mathbf{x} - \mathbf{v}_r\|^2}{\|\mathbf{x} - \mathbf{v}_\ell\|^2}\right)^2 \left(\frac{\|\mathbf{x} - \mathbf{v}_\ell\|^2}{D_p(\mathbf{x})}\right)^{1+p}, \quad 1 \leq \ell \leq c. \tag{17}$$

The proposed formulation leads to infinitely many LVQ algorithms as p spans the interval $(-\infty, 0)$. The selection of $p \in$

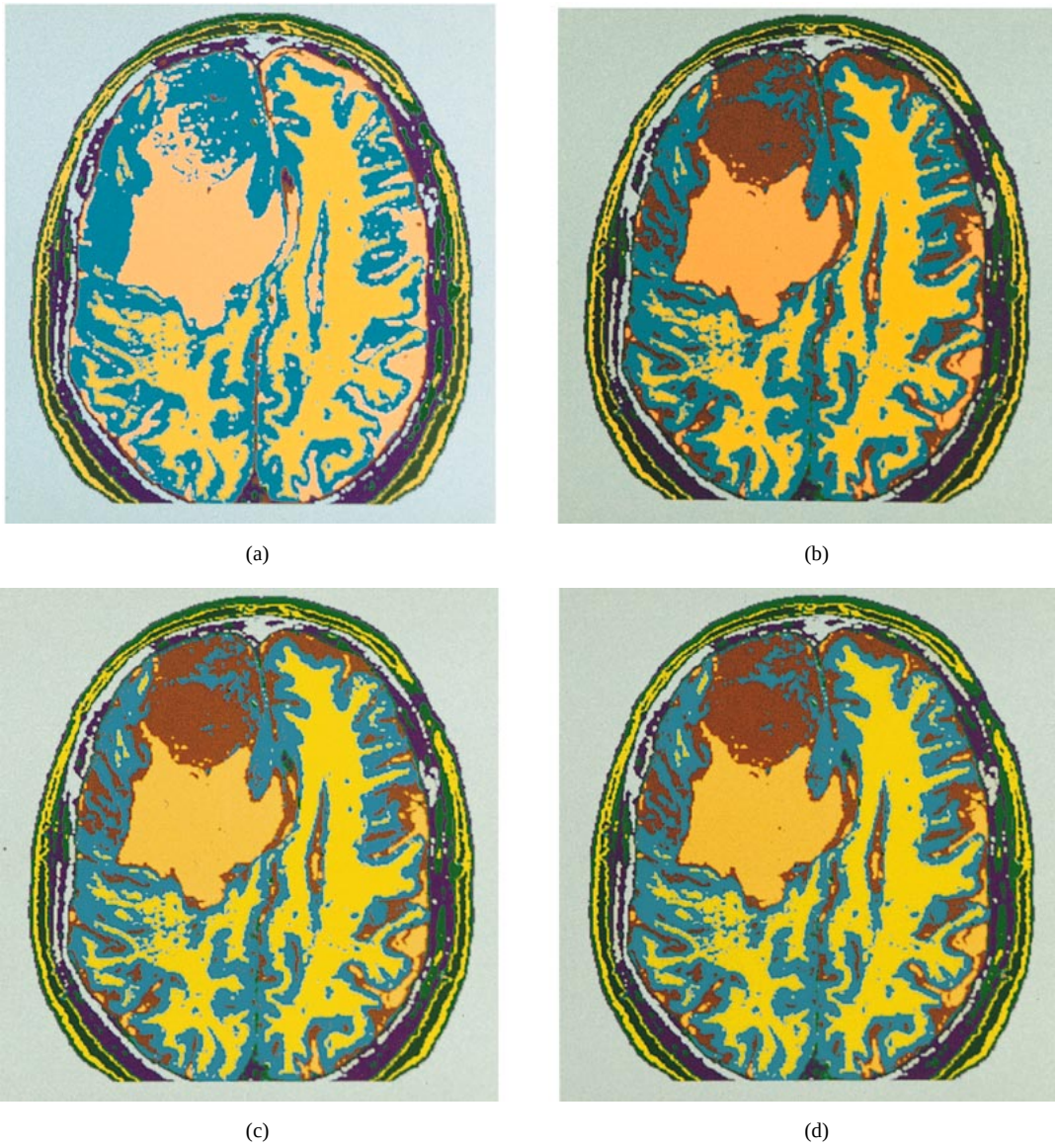

(a) (b) (c) (d)

Fig. 4. Segmented MR images produced by (a) Kohonen's (unlabeled data) LVQ algorithm; (b) the algorithm from the FALVQ 1 family corresponding to $\alpha = 1$; (c) the algorithm from the FALVQ 2 family corresponding to $\beta = 1$; and (d) the algorithm from the FALVQ 3 family corresponding to $\gamma = 1$.

$(-\infty, 0)$ affects the interference function (17) through the term $(\|\mathbf{x} - \mathbf{v}_\ell\|^2/D_p(\mathbf{x}))^{1+p}$ [10]. The interference function $w_{ir}(\mathbf{v}_i)$ represents the effect of the nonwinning prototype $\mathbf{v}_r \neq \mathbf{v}_i$ on the update of the winning prototype. The cumulative effect of all winning prototypes is represented in (15) by the sum $(1/c)\sum_{r\neq i}^{c} w_{ir}(\mathbf{v}_i)$. The behavior of the interference function $w_{ir}(\mathbf{v}_i)$ for values of $p \in (-\infty, 0)$ revealed that the update of the winning prototypes is increasingly inhibited by the nonwinning prototypes as p increases from $-\infty$ to zero [10]. Similar inferences can be made from the update equation (16) for the nonwinning prototypes. In this case, u_{ij}^2 represents the effect of the winning prototype $\mathbf{v}_i$ on the update of the nonwinning prototype $\mathbf{v}_j$. The properties of the interference function $w_{ir}(\mathbf{v}_j)$ indicated that the nonwinning prototypes are allowed to compete more strongly with the winning prototype as p increases from $-\infty$ to zero [10].

1) FALVQ 1: Consider that LVQ is based on the minimization of the loss function (2), where $u_r(\mathbf{x}) = u_{ir}$ is given by (12) with $D(\mathbf{x}) = D_p(\mathbf{x})$ and $p \to -\infty$. Since $\lim_{p\to-\infty} D_p(\mathbf{x}) = D_{\min}(\mathbf{x}) = \|\mathbf{x} - \mathbf{v}_i\|^2$, (12) approaches

$$u_{ir} = \begin{cases} 1, & \text{if } r = i \\ \left(1 + \dfrac{\|\mathbf{x} - \mathbf{v}_r\|^2}{\|\mathbf{x} - \mathbf{v}_i\|^2}\right)^{-1}, & \text{if } r \neq i. \end{cases} \tag{18}$$

If $r \neq i$, then $\|\mathbf{x} - \mathbf{v}_r\|^2/\|\mathbf{x} - \mathbf{v}_i\|^2 > 1$ and, therefore, $u_{ir} < 1/2$. Since $u_{ir} \in (0, 1/2), \forall\, r \neq i$, the function u_{ir} defined in (18) favors rather strongly the winning prototype.

The Minimum FALVQ 1, or simply FALVQ 1, can be obtained as a special case of the Generalized FALVQ 1 if $p \to -\infty$. The interference function can be determined from (17) at the limit $p \to -\infty$ as

$$w_{ir}(\mathbf{v}_\ell) = \begin{cases} c(1 - u_{ir})^2, & \text{if } \ell = i \\ 0, & \text{if } \ell \neq i. \end{cases} \tag{19}$$

If $\mathbf{x}$ is the input vector, then the winning prototype $\mathbf{v}_i$ can be updated by

$$\Delta\mathbf{v}_i = \eta(\mathbf{x} - \mathbf{v}_i)\left(1 + \sum_{r\neq i}^{c}(1 - u_{ir})^2\right) \tag{20}$$

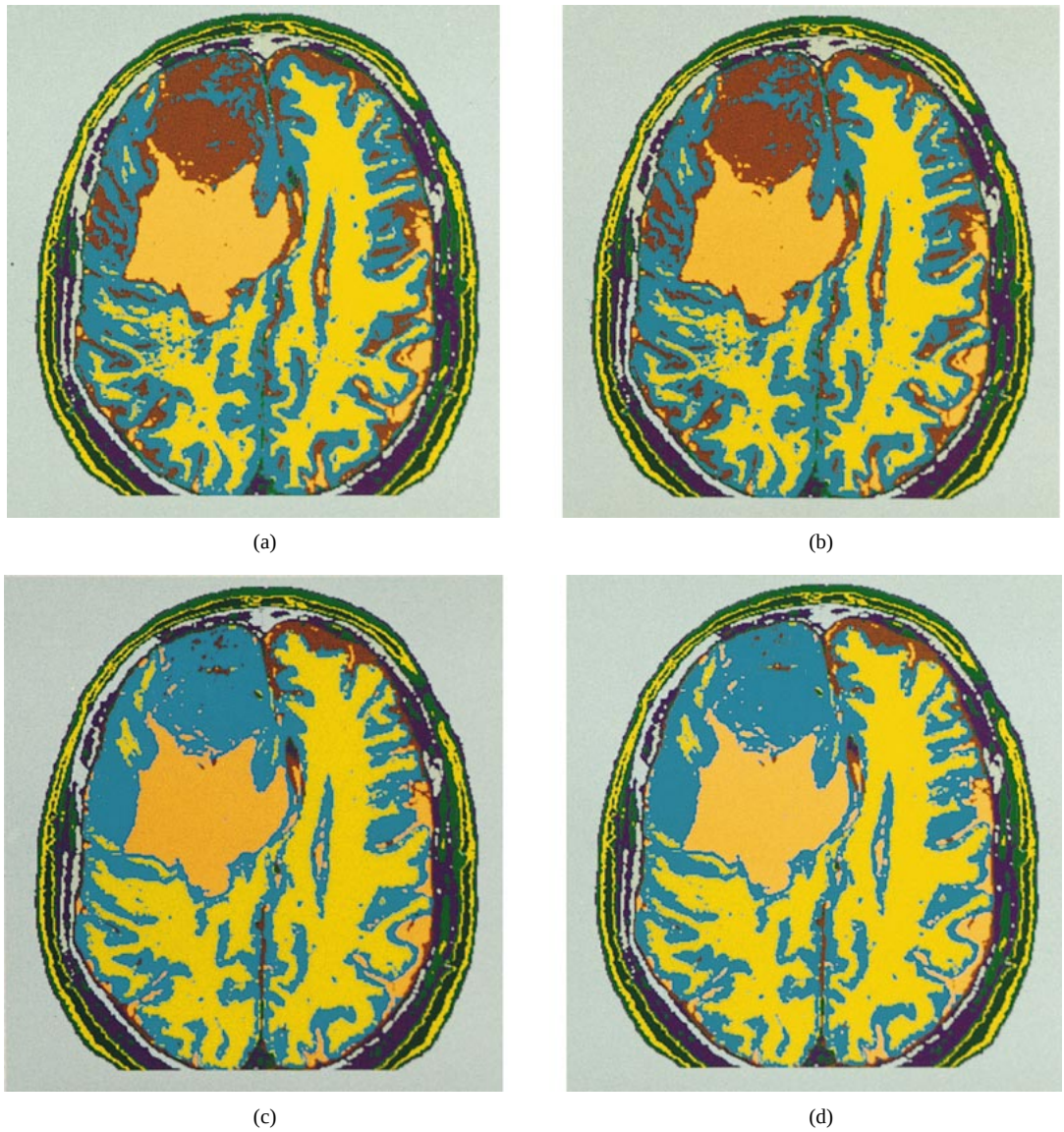

(a) (b) (c) (d)

Fig. 5. Segmented MR images by algorithms from the FALVQ 1 family with (a) $\alpha = 1$, (b) $\alpha = 0.7$, (c) $\alpha = 0.5$, and (d) $\alpha = 0.1$.

while the nonwinning prototypes $\mathbf{v}_j \neq \mathbf{v}_i$ can be updated by

$$\Delta \mathbf{v}_j = \eta(\mathbf{x} - \mathbf{v}_j) u_{ij}^2. \tag{21}$$

2) Harmonic FALVQ 1:

Consider that LVQ is based on the minimization of the loss function (2) where $u_r(\mathbf{x}) = u_{ir}$ is given by (12) with $D(\mathbf{x}) = D_p(\mathbf{x})$ and $p = -1$. For $p = -1$, $D_p(\mathbf{x})$ becomes the harmonic mean $D_H(\mathbf{x})$ defined as

$$\frac{1}{D_H(\mathbf{x})} = \frac{1}{c} \sum_{j=1}^{c} \frac{1}{\|\mathbf{x} - \mathbf{v}_j\|^2}. \tag{22}$$

The Harmonic FALVQ 1 can be obtained as a special case of the Generalized FALVQ 1 if $p = -1$. In this case, the interference function (17) becomes

$$w_{ir}(\mathbf{v}_\ell) = u_{ir}^2 \left(\frac{\|\mathbf{x} - \mathbf{v}_r\|^2}{\|\mathbf{x} - \mathbf{v}_\ell\|^2} \right)^2, \qquad 1 \leq \ell \leq c. \tag{23}$$

If $\mathbf{x}$ is the input vector, then the winning prototype $\mathbf{v}_i$ can be updated by

$$\Delta \mathbf{v}_i = \eta(\mathbf{x} - \mathbf{v}_i) \left(1 + \frac{1}{c} \sum_{r \neq i}^{c} u_{ir}^2 \left(\frac{\|\mathbf{x} - \mathbf{v}_r\|^2}{\|\mathbf{x} - \mathbf{v}_i\|^2} \right)^2 \right) \tag{24}$$

while the nonwinning prototypes $\mathbf{v}_j \neq \mathbf{v}_i$ can be updated by

$$\Delta \mathbf{v}_j = \eta(\mathbf{x} - \mathbf{v}_j) \left(u_{ij}^2 + \frac{1}{c} \sum_{r \neq i}^{c} u_{ir}^2 \left(\frac{\|\mathbf{x} - \mathbf{v}_r\|^2}{\|\mathbf{x} - \mathbf{v}_j\|^2} \right)^2 \right). \tag{25}$$

3) Geometric FALVQ 1: Consider that LVQ is based on the minimization of the loss function (2) where $u_r(\mathbf{x}) = u_{ir}$ is given by (12) with $D(\mathbf{x}) = D_p(\mathbf{x})$ and $p \to 0$. As $p \to 0$, $D_p(\mathbf{x})$ approaches the geometric mean $D_G(\mathbf{x})$, defined as

$$D_G(\mathbf{x}) = \left(\prod_{j=1}^{c} \|\mathbf{x} - \mathbf{v}_j\|^2 \right)^{1/c}. \tag{26}$$

The Geometric FALVQ 1 can be obtained as a special case of the Generalized FALVQ 1 if $p \to 0$. The interference function can be determined from (17) at the limit $p \to 0$ as

$$w_{ir}(\mathbf{v}_\ell) = u_{ir}(1 - u_{ir}) \frac{\|\mathbf{x} - \mathbf{v}_r\|^2}{\|\mathbf{x} - \mathbf{v}_\ell\|^2}, \qquad 1 \leq \ell \leq c. \tag{27}$$

If $\mathbf{x}$ is the input vector, then the winning prototype $\mathbf{v}_i$ can be updated

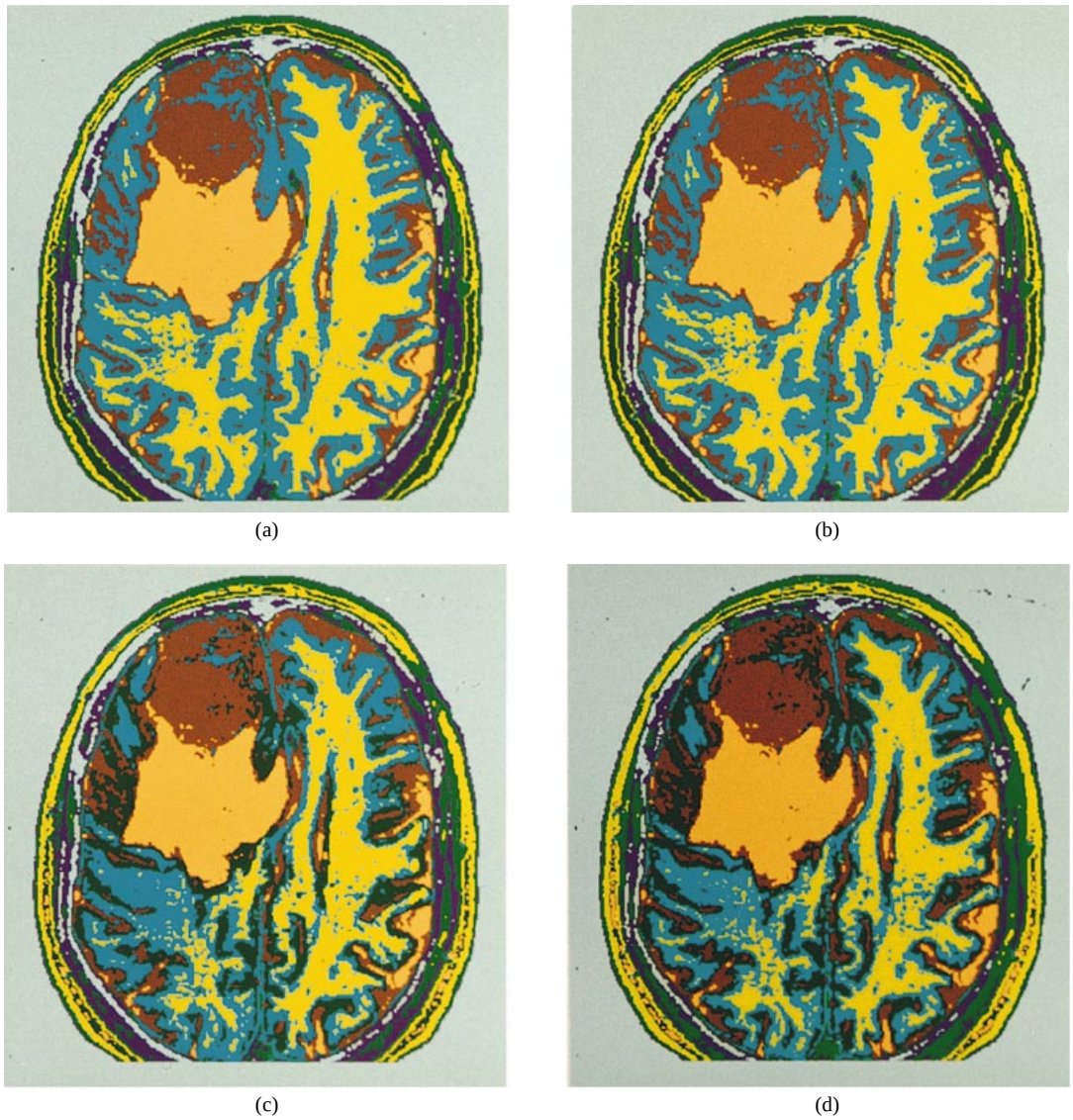

(a) (b) (c) (d)

Fig. 6. Segmented MR images by Generalized FALVQ 1 algorithms with (a) $p \rightarrow -\infty$ (FALVQ 1), (b) $p = -10$, (c) $p = -2$, and (d) $p = -1$ (Harmonic FALVQ 1).

by

$$\Delta \mathbf{v}_i = \eta(\mathbf{x} - \mathbf{v}_i)\left(1 + \frac{1}{c}\sum_{r \neq i}^{c} u_{ir}(1 - u_{ir})\frac{\|\mathbf{x} - \mathbf{v}_r\|^2}{\|\mathbf{x} - \mathbf{v}_i\|^2}\right) \tag{28}$$

while the nonwinning prototypes $\mathbf{v}_j \neq \mathbf{v}_i$ can be updated by

$$\Delta \mathbf{v}_j = \eta(\mathbf{x} - \mathbf{v}_j)\left(u_{ij}^2 + \frac{1}{c}\sum_{r \neq i}^{c} u_{ir}(1 - u_{ir})\frac{\|\mathbf{x} - \mathbf{v}_r\|^2}{\|\mathbf{x} - \mathbf{v}_j\|^2}\right). \tag{29}$$

III. Experimental Results

Fig. 3(a)–(c) shows the T1-weighted, T2-weighted, and SD MR images, respectively, of an individual with meningioma. Meningiomas are the most common form of intracranial tumors. In this case, the tumor is located in the right frontal lobe (upper-left quarter of the MR images) and appears bright on the T2-weighted image and dark on the T1-weighted image. The tumor appears very bright and isolated from surrounding tissue in Fig. 3(d), which shows the T1-weighted MR image recorded after the patient was given Gadolinium. There is also a large amount of edema surrounding the tumor, which appears very bright on the T2-weighted image shown in Fig. 3(b).

The MR image shown in Fig. 3 was segmented using Kohonen's (unlabeled data) LVQ algorithm and algorithms from the FALVQ 1, FALVQ 2, and FALVQ 3 families. In these experiments, the feature vectors were formed using the pixel values of the T1-weighted, T2-weighted, and SD images shown in Fig. 3(a)–(c), respectively. Fig. 3(d), which shows the T1-weighted image with Gadolinium, was used to evaluate the segmented images since the tumor appears very bright and is well separated from surrounding tissue. In all these experiments, $c = 8$, that is, the segmented images contained eight different segments which were artificially colored. Fig. 4(a) shows the segmented image produced by Kohonen's (unlabeled data) LVQ algorithm applied with $N = 100$ and initial value of the learning rate $\eta_0 = 0.1$. It was found that the algorithm achieves its best performance for initial values of the learning rate in the range 0.1–0.9. Kohonen's (unlabeled data) LVQ algorithm succeeded in identifying the edema, but failed to separate the tumor from surrounding tissue. Fig. 4(b) shows the segmented image produced by the algorithm from the FALVQ 1 family corresponding to $\alpha = 1$ (competition measures: $A_u = 0.306$, $C_u = 0.629$). Fig. 4(c) shows the segmented image produced by the algorithm from the FALVQ 2 family corresponding to $\beta = 1$ (competition measures: $A_u = 0.264$, $C_u = 0.608$). Fig. 4(d)

shows the segmented image produced by the algorithm from the FALVQ 3 family corresponding to $\gamma = 1$ (competition measures: $A_u = 0.167$, $C_u = 0.5$). In all of these experiments the initial value of the learning rate was $\eta_0 = 0.001$ and the total number of iterations was $N = 100$. The tumor and the surrounding edema were clearly identified by all three algorithms from the FALVQ 1, FALVQ 2, and FALVQ 3 families tested in these experiments.

The competition between the prototypes during learning and its impact on the performance of FALVQ algorithms were further explored by an additional set of experiments, which evaluated the effect of the free parameter α on the performance of various algorithms from the FALVQ 1 family. Fig. 5(a)–(d) shows the segmented images produced by algorithms from the FALVQ 1 family with $\alpha = 1$ (competition measures: $A_u = 0.306$, $C_u = 0.629$), $\alpha = 0.7$ (competition measures: $A_u = 0.346$, $C_u = 0.638$), $\alpha = 0.5$ (competition measures: $A_u = 0.378$, $C_u = 0.644$), and $\alpha = 0.1$ (competition measures: $A_u = 0.469$, $C_u = 0.661$), respectively. In all these of experiments the initial value of the learning rate was $\eta_0 = 0.001$ and the total number of iterations was $N = 100$. The algorithms from the FALVQ 1 family failed to separate the tumor from surrounding tissue as the value of α decreased below 0.7. In fact, the algorithms corresponding to $\alpha = 0.5$ and $\alpha = 0.1$ resulted in segmented images very similar to that produced by Kohonen's (unlabeled data) LVQ algorithm that allows only the winning prototype to be updated in order to match the input vector. Moreover, there are no visible differences between the segmented images produced by FALVQ 1 algorithms for $\alpha = 0.7$ and $\alpha = 1.0$. It was also observed that increasing the value of α above 1.0 had no significant effect on the segmented images until α reached values above ten. Finally, the performance of the algorithms from this family is in perfect agreement with the behavior of the competition measures A_u and C_u as the value of α changes.

The last set of experiments evaluated the performance of Generalized FALVQ 1 algorithms. Fig. 6(a)–(d) shows the segmented images produced by the Generalized FALVQ 1 algorithms with $p \to -\infty$ (FALVQ 1), $p = -10$, $p = -2$, and $p = -1$ (Harmonic FALVQ 1), respectively. Increasing the value of p from $-\infty$ to -1 required a decrease in the initial value η_0 of the learning rate. Clearly, the Harmonic FALVQ 1 and FALVQ 1 algorithms resulted in segmented images with remarkable differences. For example, the two algorithms exhibit different behavior in areas occupied by different types of normal tissue. Nevertheless, they both succeeded in separating the tumor from normal tissues. The segmented image obtained with $p = -2$ is very close to that produced by the Harmonic FALVQ 1 algorithm ($p = -1$) while the segmented image obtained with $p = -10$ resembles that produced by the FALVQ 1 algorithm ($p \to -\infty$). In fact, the Generalized FALVQ 1 algorithms behaved like the Harmonic FALVQ 1 algorithm for values of p in a relatively small neighborhood of $p = -1$, while their behavior was closer to that of the FALVQ 1 algorithm as the value of p decreased. The behavior of Generalized FALVQ 1 algorithms in these experiments verifies that the effect of the free parameter p on their performance is highly nonlinear. This is in full agreement with the behavior of the generalized mean $D_p(\mathbf{x})$ for different values of $p \in (-\infty, 0)$.

IV. Conclusions

This paper presented the evaluation of a segmentation technique for MR images of the brain based on FALVQ algorithms. This segmentation approach is simple and easily implementable, while the use of unsupervised LVQ algorithms does not rely on *a priori* information provided by human experts. It was experimentally verified that the LVQ algorithms tested were successful in differentiating between normal and abnormal tissues when the nonwinning prototypes were allowed to compete with the winning prototype to match each input vector of the LVQ network. The experiments also indicated that the competition measures presented in this paper are fully consistent with the behavior of the algorithms in practice. It is remarkable that the performance of FALVQ algorithms degraded considerably in the limit where their behavior approaches that of Kohonen's (unlabeled data) LVQ, which allows only the winning prototype to be updated. The experiments revealed the ability of all Generalized FALVQ 1 algorithms tested to discriminate between normal tissues and abnormalities. This is an indication that the Generalized FALVQ 1 algorithms are interesting alternatives to the original FALVQ families of algorithms.

References

[1] J. C. Bezdek, *Pattern Recognition with Fuzzy Objective Function Algorithms.* New York: Plenum, 1981.

[2] M. Bomans, K.-H. Hohne, U. Tiede, and M. Riemer, "3-D segmentation of MR images of the head for 3-D display," *IEEE Trans. Med. Imag.*, vol. 9, pp. 177–183, June 1990.

[3] L. P. Clarke, "MR image segmentation using MLM and artificial neural nets," *Medical Physics*, vol. 18, no. 3, p. 673, 1991.

[4] A. Gersho and R. M. Gray, *Vector Quantization and Signal Compression.* Boston, MA: Kluwer, 1992.

[5] L. O. Hall, A. M. Bensaid, L. P. Clarke, R. P. Velthuizen, M. S. Silbiger, and J. C. Bezdek, "A comparison of neural network and fuzzy clustering techniques in segmenting magnetic resonance images of the brain," *IEEE Trans. Neural Networks*, vol. 3, pp. 672–682, Sept. 1992.

[6] R. M. Haralick and L. G. Shapiro, "Image segmentation techniques," *Comput. Vision, Graph., Image Processing*, vol. 29, pp. 100–132, 1985.

[7] E. C. Hildreth, "The detection of intensity changes by computer and biological vision systems," *Comput. Vision, Graph., Image Processing*, vol. 22, pp. 1–27, 1983.

[8] T. J. Hyman, R. J. Kurland, G. C. Levy, and J. D. Shoop, "Characterization of normal brain tissue using seven calculated MRI parameters and a statistical analysis system," *Magnetic Resonance Med.*, vol. 11, pp. 22–34, 1989.

[9] N. B. Karayiannis, "Generalized fuzzy c-means algorithms," in *Proc. Fifth Int. Conf. Fuzzy Systems*, New Orleans, LA, Sept. 8–11, 1996, pp. 1036–1042.

[10] N. B. Karayiannis, "Learning vector quantization: A review," *Int. J. Smart Eng. Syst. Design*, vol. 1, pp. 33–58, 1997.

[11] ——, "Fuzzy partition entropies and entropy constrained clustering algorithms," *J. Intell. Fuzzy Syst.*, vol. 5, no. 2, pp. 103–111, 1997.

[12] ——, "A methodology for constructing fuzzy algorithms for learning vector quantization," *IEEE Trans. Neural Networks*, vol. 8, pp. 505–518, May 1997.

[13] N. B. Karayiannis, J. C. Bezdek, N. R. Pal, R. J. Hathaway, and P.-I Pai, "Repairs to GLVQ: A new family of competitive learning schemes," *IEEE Trans. Neural Networks*, vol. 7, pp. 1062–1071, Sept. 1996.

[14] N. B. Karayiannis and J. C. Bezdek, "An integrated approach to fuzzy learning vector quantization and fuzzy c-means clustering," *IEEE Trans. Fuzzy Syst.* , vol. 5, pp. 622–628, Nov. 1997.

[15] N. B. Karayiannis and P.-I Pai, "A family of fuzzy algorithms for learning vector quantization," *Intelligent Engineering Systems Through Artificial Neural Networks*, C. H. Dagli *et al.*, Eds. New York: ASME, 1994, vol. 4, pp. 219–224.

[16] ——, "Fuzzy algorithms for learning vector quantization," *IEEE Trans. Neural Networks*, vol. 7, pp. 1196–1211, Sept. 1996.

[17] T. Kohonen, *Self-Organization and Associative Memory*, 3rd ed. Berlin, Germany: Springer-Verlag, 1989.

[18] N. R. Pal, J. C. Bezdek, and E. C.-K. Tsao, "Generalized clustering networks and Kohonen's self-organizing scheme," *IEEE Trans. Neural Networks*, vol. 4, pp. 549–557, July 1993.

[19] S. P. Raya, "Low-level segmentation of 3-D magnetic resonance brain images—A rule-based system," *IEEE Trans. Med. Imag.*, vol. 9, pp. 327–337, Sept. 1990.

[20] D. E. Rumelhart, G. E. Hinton, and R. J. Williams, "Learning internal representations by error propagation," *Parallel Distributed Processing*, D. E. Rumelhart and J. L. McClelland, Eds. Cambridge, MA: MIT, 1986, vol. I, pp. 318–362.

[21] J. Serra, *Image Analysis and Mathematical Morphology.* London, U.K.: Academic, 1982.

[22] E. C.-K. Tsao, J. C. Bezdek, and N. R. Pal, "Fuzzy Kohonen clustering networks," *Patt. Recognit.*, vol. 27, no. 5, pp. 757–764, 1994.